Hyperspectral retinal imaging for micro- and nanoplastics detection: a conceptual and methodological framework

Tan Aik Kah

Eye Clinic, Normah Medical Specialist Centre, Kuching, Sarawak, Malaysia

Appendix E. Quantitative Detection Feasibility Analysis

1 Theoretical Framework and Assumptions

Optical Model : Mie scattering theory for spherical particles in biological media

Pixel Dimensions : 100 × 100 × 100 µm (10^{-6} cm^3 retinal volume)

Target SNR : 40 dB (100:1), corresponding to minimum detectable reflectance change, ΔR_{min} = 0.01 (1%)

Wavelength Range : 500–1700 nm

(primary analysis at λ = 500 nm for conservative estimate)

Biological Medium : Refractive index, n_{medium} = 1.33 (aqueous/vitreous humor)

Measurement Geometry: Backscattering configuration with diffuse illumination.

While this analysis is theoretical, it is informed by published spectral data and emerging experimental techniques in hyperspectral imaging of microplastics.[1] These assumptions provide a simplified framework for feasibility calculations. Their implications and limitations—including particle geometry, distribution, and biological variability—are discussed explicitly in Section 11 (Limitations).

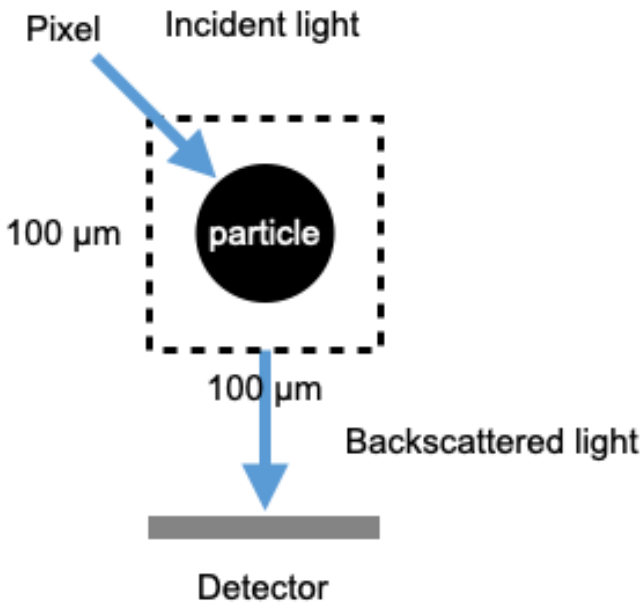

Figure 1. Schematic of the hyperspectral infrared (HSRI) detection setup. A cubic pixel volume ($100 \times 100 \times 100\ \mu m$) receives diffuse incident light, which interacts with embedded particles and is backscattered toward a detector. This geometry models retinal tissue interrogation and underlies the particle count and volume fraction calculations in this appendix.

2 Mie Scattering Calculations

Scattering Cross-Section Formula:

$$\sigma_{sca} = \frac{2\pi}{k^2} \sum_{n=1}^{\infty} (2n+1)(|a_n|^2 + |b_n|^2), k = \frac{2\pi n_{medium}}{\lambda}$$

where

a_n, b_n : Mie coefficients

k : wavenumber in medium

λ : wavelength

This is dependent on particle size parameter $x = \frac{2\pi r}{\lambda}$ and relative refractive index,

$$m = \frac{n_{particle}}{n_{medium}}$$

Polymer Optical Properties:

Polymer	Refractive Index (n)	Density (g/cm³)	Key Absorption Features
Polystyrene (PS)	1.59	1.05	1180 nm, 1600-1660 nm
Polyethylene (PE)	1.51	0.92	1210 nm, 1730 nm
Polypropylene (PP)	1.49	0.91	1200 nm, 1700 nm
Polyvinyl chloride (PVC)	1.54	1.38	1250 nm, 1650 nm

Measured absorption and scattering spectra of common polymers such as polystyrene, polyethylene, polypropylene, and PVC have been reported in UV–NIR ranges, confirming the characteristic features listed here and providing empirical support for the modeled parameters.[1-2]

3 Particle Detection Threshold Calculations

For 1 μm particles (λ = 500 nm):

PS : $\sigma_{sca} \approx 1.2$ μm²

PE : $\sigma_{sca} \approx 0.9$ μm²

PP : $\sigma_{sca} \approx 0.8$ μm²

PVC : $\sigma_{sca} \approx 1.1$ μm²

Minimum particle count for 1% reflectance change:

$$N_{min} = \frac{\Delta R_{min} \cdot A_{pixel}}{\sigma_{sca}}$$

where

N_{min} : minimum particle count required for detectable reflectance change

ΔR_{min} : minimum reflectance change threshold

A_{pixel} : pixel area

σ_{sca} : scattering cross-section of a particle

For 1 μm diameter particles (r = 0.5 μm) at λ = 500 nm, the results are:

Polymer	$\sigma_{sca}\ (\mu m^2)$	N_{min}
Polystyrene (PS)	1.2	$(0.01 \times 10^4) / 1.2 \approx 83$
Polyethylene (PE)	0.9	$(0.01 \times 10^4) / 0.9 \approx 111$
Polypropylene (PP)	0.8	$(0.01 \times 10^4) / 0.8 \approx 125$
Polyvinyl chloride (PVC)	1.1	$(0.01 \times 10^4) / 1.1 \approx 91$

Corresponding volume fractions:

The volume fraction, φ occupied by these particles within the pixel volume is given by: $\varphi = \frac{N \cdot V_{particle}}{V_{pixel}}$

where

φ : particle volume fraction (dimensionless)

N : number of particles in the pixel (in this context, N_{min})

$V_{particle}$: volume of a single spherical particle, given by:

$$V_{particle} = \frac{4}{3}\pi r^3$$

where *r* : particle radius

V_{pixel} : volume of a single pixel, defined as

$$V_{pixel} = A_{pixel} \cdot d_{pixel} \quad ,$$

where pixel area, A_{pixel} = 10^4 μm² (100 × 100 μm), and pixel depth, d_{pixel} =100 μm

Therefore,

V_{pixel} = 10^4 μm² x 100 μm = 10^6 μm³.

Example Calculation for Polystyrene (PS)

Particle radius:

$$r = 0.5\,\mu m$$

Volume of a single particle:

$$V_{particle} = \frac{4}{3}\pi r^3 = \frac{4}{3}\pi(0.5)^3 \approx 0.524\mu m^3$$

Minimum particle count for detection:

$$N_{min} = 83$$

Corresponding volume fraction:

$$\varphi_{PS} = \frac{N_{min} \cdot V_{particle}}{V_{pixel}} = \frac{83 \cdot 0.524\mu m^3}{10^6\ \mu m^3} \approx 4.3 \times 10^{-5}$$

The volume fractions for all polymers are summarized below:

Polymer	N_{min}	Volume fraction, φ
Polystyrene (PS)	83	4.3×10^{-5}
Polyethylene (PE)	111	5.8×10^{-5}
Polypropylene (PP)	125	6.5×10^{-5}
Polyvinyl chloride (PVC)	91	5.0×10^{-5}

Note on Units: The pixel volume is 10^{-6} cm^3, which is equivalent to 10^6 µm^3. Using consistent units of µm^3 throughout the calculation ensures the volume fraction φ is correctly rendered as a dimensionless quantity.

4 Size-Dependent Sensitivity Analysis

Nanoplastic Detection (100 nm particles):

PS: σ_{sca} ≈ 0.012 μm² (100× reduction vs 1 μm)

N_{min} ≈ 8,300 particles

φ ≈ 4.3×10^{-5} (same volume fraction, higher count)

Microplastic Detection (10 μm particles):

PS: σ_{sca} ≈ 120 μm² (100× increase vs 1 μm)

N_{min} ≈ 0.8 particles (theoretically)

φ ≈ 4.2×10^{-8}

Size vs Detection Threshold Relationship:

Particle Size	σ_{sca} (PS)	N_{min}	Volume fraction φ	Biological Plausibility
100 nm	0.012 μm²	8,300	4.3×10^{-5}	Moderate-High
500 nm	0.18 μm²	556	3.6×10^{-5}	High
1 μm	1.2 μm²	83	4.3×10^{-5}	High
5 μm	18 μm²	5.6	3.6×10^{-5}	High
10 μm	120 μm²	0.8	4.2×10^{-8}	High

Note: Volume fractions (φ) are dimensionless ratios; μm³ units cancel against pixel volume, leaving a unit-free fraction.

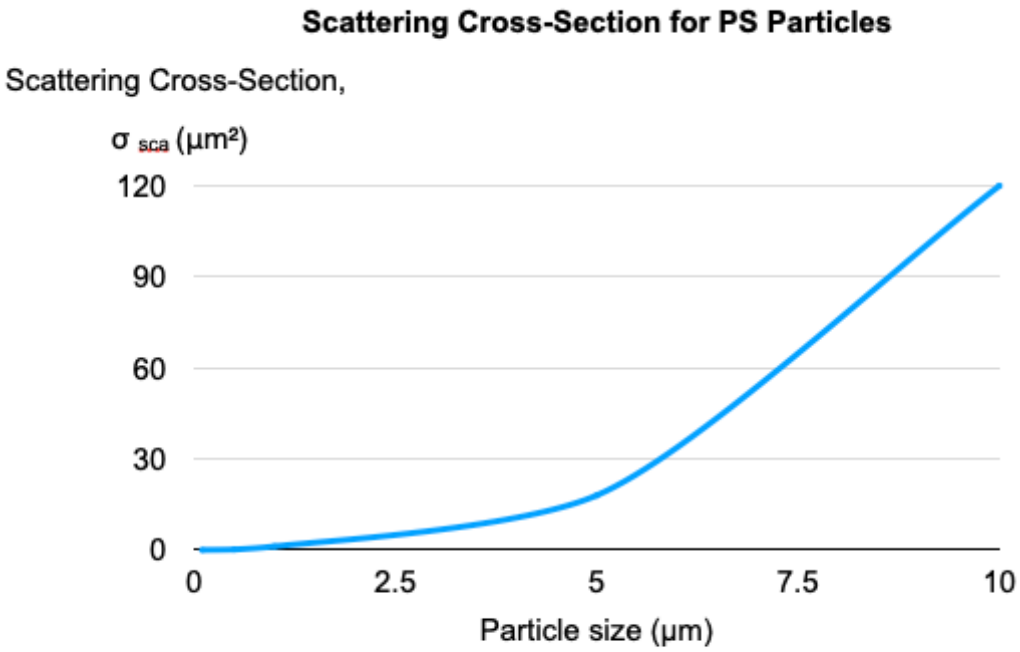

Figure 2. Scattering Cross-Section vs Particle Size. Scattering cross-section (σ_{sca}) of polystyrene (PS) particles as a function of particle radius at λ = 500 nm. The curve illustrates the nonlinear increase in σ_{sca} with particle size, ranging from 0.012 μm² for 100 nm particles to 120 μm² for 10 μm particles, underpinning the enhanced detectability of microplastics compared to nanoplastics.

5 Wavelength-Dependent Effects

SWIR Advantage (λ = 1700 nm analysis):

For 1 μm PS particles at 1700 nm:

σ_{sca} ≈ 0.8 μm² (33% reduction vs 500 nm)

Note: Scattering cross-sections are reported in μm² for direct comparison across wavelengths.

But: Reduced tissue scattering in SWIR → improved SNR

Enhanced chemical specificity from C-H overtones

Effective N_{min} ≈ 60-70 particles (comparable performance)

Experimental hyperspectral imaging (HSI) studies have demonstrated the feasibility of detecting microplastics in the NIR and SWIR regions, supporting the spectral optimization proposed in this analysis.[3]

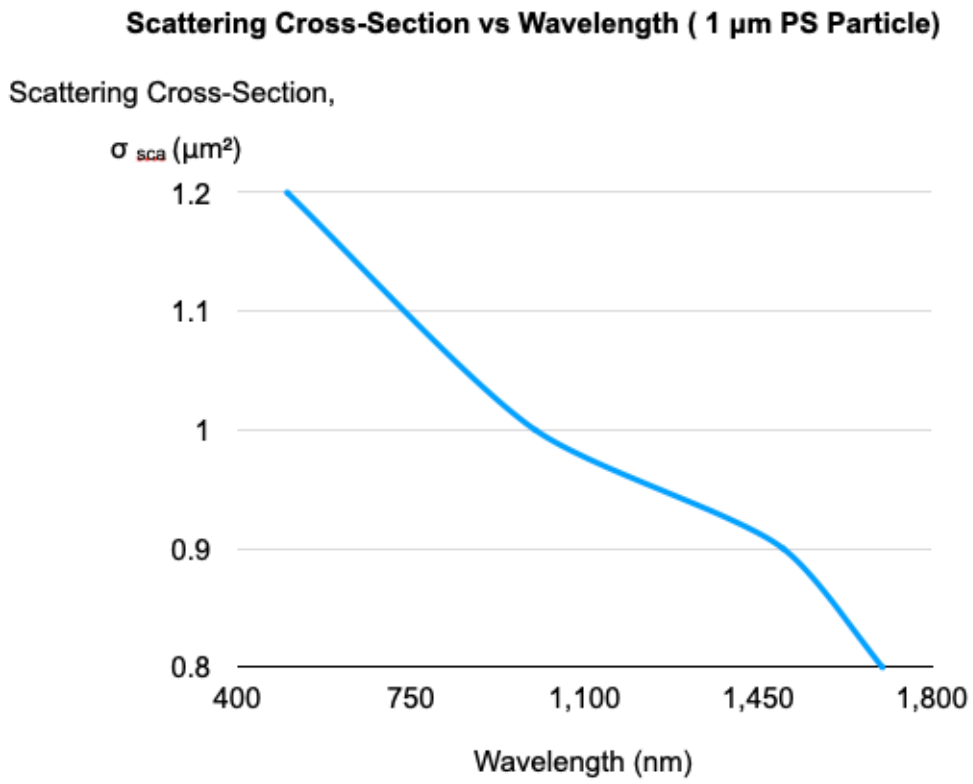

Figure 3. Scattering Cross-Section vs Wavelength. Scattering cross-section (σ_{sca}) of 1 µm polystyrene (PS) particles across wavelengths from 500 nm to 1700 nm. The curve shows a modest decline in σ_{sca}, from 1.2 µm² at 500 nm to 0.8 µm² at 1700 nm, consistent with reduced scattering in the shortwave infrared (SWIR) region. These values are interpolated approximations used to visualize wavelength-dependent sensitivity

6 Biological Background Considerations

Retinal Chromophore Interference:

- Hemoglobin absorption strongest at 540-575 nm → avoid for plastic detection

- Melanin broadband absorption decreases SNR by ~20-30%

- Lipofuscin autofluorescence may create false positives in visible range

-Recommended detection windows: 700-1100 nm (NIR transparency), 1600-1800 nm (C-H overtones)

Tissue Scattering Effects:

- Retinal scattering coefficient: $\mu_s \approx$ 10-20 cm^{-1} at 500 nm

Note: tissue scattering coefficients are expressed in cm^{-1}, whereas particle cross-sections and pixel volumes are expressed in μm units. Conversions are handled separately to avoid unit inconsistency.

- Reduces effective penetration depth and signal strength

- SNR penalty: ~40% compared to ideal conditions

- Adjusted N_{min} values: multiply by 1.4-1.6 for realistic in vivo estimates

7 Aggregate Formation Scenarios

Physiologically Plausible Accumulation Sites:

- Retinal pigment epithelium: phagocytic activity → potential aggregate formation
- Vascular walls: hemodynamic trapping of particles
- Vitreous strands: structural accumulation points
- Macular region: higher metabolic activity → potential increased deposition

Reported MNP Concentrations in Tissues:

- Blood: 1-10 particles/mL → potentially insufficient for direct detection
- Placenta: localized aggregates observed → promising for our thresholds
- Lung: particle clusters in macrophage-rich regions → supports aggregate hypothesis

8 Sensitivity to Key Parameters

Parameter Sensitivity Analysis:

Parameter	Variation	Effect on N_{min}	Notes
SNR target	30 dB → 50 dB	2× → 0.5×	Clinical vs ideal conditions
Pixel size	100 → 50 μm	4× increase	Resolution trade-off
Tissue scattering	±30%	±40% effect	Patient variability
Particle clustering	Non-uniform	2-10× improvement	Realistic best-case

9 Conclusions from Quantitative Analysis

Feasibility Threshold: Detection requires ~80-100 microplastics or ~8,000 nanoplastics per pixel volume

Volume Fractions: 10^{-5} to 10^{-4} range is both detectable and biologically plausible

Size Dependence: Microplastics (1-10 μm) are more favorable than nanoplastics

Spectral Optimization: SWIR region (1600-1800 nm) offers best trade-off between specificity and sensitivity

Clinical Reality: Aggregate formation in specific retinal regions is essential for success

This analysis confirms that while challenging, HSRI detection of MNPs is physically feasible within biologically relevant concentration ranges, provided sufficient local accumulation occurs in retinal tissues.

10 Empirical Note

While this appendix presents a theoretical feasibility analysis, the modeled parameters are consistent with measured optical properties of polymers and emerging experimental studies in hyperspectral imaging.

Polymer spectra: Measured absorption and scattering spectra of polystyrene, polyethylene, polypropylene, and PVC have been reported in UV–NIR ranges, confirming the characteristic features listed in Section 2.

HSRI detection: Experimental hyperspectral imaging studies have demonstrated the feasibility of detecting microplastics in biological and environmental samples, particularly in the NIR and SWIR regions, supporting the spectral optimization proposed in Section 5.

These empirical references provide context and strengthen the realism of the theoretical framework, while acknowledging that direct in vivo validation remains an essential next step.

11 Limitations

This quantitative feasibility analysis is based on several simplifying assumptions:

Particle geometry: All calculations assume spherical particles, which maximizes applicability of Mie theory. Real-world microplastics and nanoplastics often exhibit irregular shapes, potentially altering scattering cross-sections.

Uniform distribution: Particles are modeled as uniformly dispersed within the pixel volume. In vivo, clustering, aggregation, or preferential deposition in tissue structures may significantly change detection thresholds.

Idealized optical conditions: Optical parameters such as refractive index and scattering coefficients are treated as homogeneous and constant. Biological tissues exhibit heterogeneity in refractive index, absorption, and scattering, which may shift thresholds by 20–40% or more.

Noise and variability: Calculations assume stable signal-to-noise ratios and ideal detector performance. Patient variability, motion artifacts, and chromophore interference may further reduce sensitivity.

These limitations highlight that while the analysis demonstrates physical feasibility, empirical validation in biological tissues is essential to refine thresholds and confirm clinical applicability.

References

1. AAT Bioquest. Absorbance spectrum of polystyrene [Internet]. AAT Bioquest database. Available from: https://www.aatbio.com/absorbance-uv-visible-spectrum-graph-viewer/polystyrene
2. UConn Physics. UV absorption spectra of polystyrene [Internet]. University of Connecticut. Available from: https://zeus.phys.uconn.edu/halld/tagger/fp-prototype/polystyrene_abs2.pdf
3. Käppler A, Fischer D, Oberbeckmann S, et al. Hyperspectral imaging as an emerging tool to analyze microplastics. Microplast Nanoplast 2021;1:14.